RAA 2018 Vol. **18** No. **9**, 116(10pp) doi: 10.1088/1674–4527/18/9/116

http://www.raa-journal.org *http://iopscience.iop.org/raa*

***R**esearch in*
***A**stronomy and*
***A**strophysics*

NSVS 01286630: a detached binary with a close-in companion

Bin Zhang[1,2,3], Sheng-Bang Qian[1,2,3], Nian-Ping Liu[1,2,3], Wen-Ping Liao[1,2,3], Li-Ying Zhu[1,2,3], Ai-Jun Dong[4] and Qi-Jun Zhi[4]

[1] Yunnan Observatories, Chinese Academy of Sciences, Kunming 650216, China; *zhangbin@ynao.ac.cn*
[2] Key Laboratory of the Structure and Evolution of Celestial Objects, Chinese Academy of Sciences, Kunming 650216, China
[3] University of Chinese Academy of Sciences, Beijing 100049, China
[4] School of Physics and Electronic Science, Guizhou Normal University, Guiyang 550001, China

Received 2018 March 30; accepted 2018 May 13

Abstract New photometric observations of NSVS 01286630 were performed and two sets of four-color (B, V, R_c, I_c) light curves (LCs) were obtained. Using the 2013 version of the Wilson-Devinney (W–D) code, we analyzed these data. The photometric solutions reveal that NSVS 01286630 is an active detached eclipsing binary (EB) with a high orbital inclination (nearly $90°$). Remarkably, the temperature of the primary component (the hotter star) is higher than the secondary one, but the value of mass ratio $q(\frac{M_2}{M_1})$ for NSVS 0128663 is more than 1, which can be explained in that the surface of the secondary component of NSVS 01286630 is covered with big cool starspots. Based on our new CCD mid-eclipse times and the data published until now, variations in the mid-eclipse times were reanalyzed in detail using a weighted least-squares method. It is discovered that the $(O-C)$ diagram of the system shows a cyclic oscillation with a period of 3.61 yr and an amplitude of 0.001 d. The cyclic variation may be caused by the light-travel time effect (LTTE) due to the presence of a third companion, whose mass we calculated as $M_3 \sin(i_3) = 0.11\, M_\odot$. The third body may affect the orbital evolution of the central binary system by transferring angular momentum.

Key words: stars: binaries: close — stars: binaries: eclipsing — stars: individual (NSVS 01286630)

1 INTRODUCTION

A lot of close binaries form with a close-in companion, and the tertiary components play an important role in the formation and evolution of these systems (Wolf et al. 2016; Fabrycky & Tremaine 2007). Statistically studying a large sample of eclipsing binaries (EBs) is a useful way to look for evidence of hierarchical triple-star systems. The LAMOST survey released many EB data recently, including some important stellar atmospheric parameters such as effective temperature, gravitational acceleration and metallicity (Qian et al. 2017). Using these data, Qian et al. (2017) investigated the correlations between orbital period and other parameters, and found many EB candidates with a third body. Another search through the photometric database of Kepler EBs suggested that at least 20% of all close binaries have tertiary companions (Gies et al. 2012; Rappaport et al. 2013; Conroy et al. 2014; Borkovits et al. 2015, 2016). For an EB system, the presence of a tertiary component can cause a cyclical variation in the minimum light times, which can be investigated using the known $(O-C)$ method. Through analyzing the difference between observed and computed mid-eclipse times with a given ephemeris, we can obtain some orbital parameters of a third body (Liao & Qian 2010b). In other words, we can discover possible multi-systems by searching for periodic features in the observed $(O-C)$ diagram (Wolf et al. 2016). Using this method, many successful examples of the detection of a third body around close binaries have been reported in

recent years, such as V1104 Her (Liu et al. 2015), V401 Cyg (Zhu et al. 2013), V894 Cyg (Li & Qian 2014), KIC 5513861 (Zasche et al. 2015) and KIC 9532219 (Lee et al. 2016). Specifically, the stable M-type contact binary system SDSS J001641-000925 with a close-in star companion was also discovered (Qian et al. 2015b).

NSVS 01286630 (=NSVS 1135262) was first detected as an EB candidate in 2004 (Woźniak et al. 2004), and after 3 yr, the first paper about this target was published (Coughlin & Shaw 2007). The research results from Coughlin & Shaw (2007) suggested that NSVS 01286630 is a detached EB system with big cool starspots in its polar areas, which implies there is strong magnetic activity in this system. The physical masses and radiuses are also calculated based on assigned masses extrapolated from their temperature. The preliminary model seems to support the current findings that low-mass stars have a greater radius and lower effective temperature than the best models predicted (Lacy 1977). Recently, after analyzing the period variations of NSVS 01286630 using the $(O-C)$ method, the existence of a cyclic oscillation with an amplitude of 0.00105 days and a period of about 1317 days was discovered by Wolf et al. (2016). They thought that this period change may be caused by the presence of a third body, and according to their fitting parameters, the lowest mass of the third body was calculated as $0.10\,M_{\odot}$. Based on these findings, we monitored this target for several years.

In the present paper, the first four-color (B, V, R_c, I_c) light curve (LC) of NSVS 01286630 is obtained and analyzed. We also use new mid-eclipse times coupled with old data to analyze the $(O-C)$ diagram, which shows a short-term oscillation cycle because of the presence of a third body. Based on the photometric analysis and $(O-C)$ fitting results, the tertiary star, evolution state and magnetic activity of this system are discussed.

2 MULTI-COLOR CCD PHOTOMETRIC OBSERVATIONS

Two-sets of LCs in BVR_cI_c bands of NSVS 01286630 were obtained in 2010 and 2011, respectively. The first set of LCs was observed on 2010 November 2 and 3, and the second set of LCs was acquired on 2011 May 2, 5 and 6, and June 11, 12 and 20. A total of more than 1900 CCD images was recorded using the 85 cm telescope at Xinglong Station of National Astronomical Observatories, Chinese Academy of Sciences. This telescope is equipped with a 1024×1024 PI1024 BFT camera with a standard Johnson-Cousins-Bessel multicolor CCD photometric system, the effective field of view of which is 16.5 arcmin by 16.5 arcmin, corresponding to a plate scale of 0.97 arcsec pixel^{-1} (Zhou et al. 2009). From 2014 to 2015, the telescope had been upgraded by local technicians; detailed information about this process can found in Bai et al. (2018). Its filter system, mounted at the primary focus, can help to lessen optical loss and cut down the exposure time. As a consequence, the integration times in BVR_cI_c bands are 40 s, 30 s, 20 s and 10 s, respectively. Another two stars near the target with similar brightnesses were chosen as the comparison star and check star, and their coordinates are listed in Table 1.

All of the observed CCD images were reduced with IRAF[1], including flat-fielding and bias correction. By calculating the phase of the observations with a new equation, the observed LCs are plotted in Figure 1. In order to avoid the phase shift, the phase of those observations displayed in Figure 1 was calculated with our new linear ephemeris

$$\begin{aligned}\mathrm{Min.(HJD)} =& 2455504.0113(\pm0.00052)\\ &+0.38392787(\pm0.00000001)^{\mathrm{d}}\times E.\end{aligned}\tag{1}$$

In addition, new CCD times of light minima for NSVS 01286630 were also observed and determined. These are listed in Table 2.

3 ORBITAL PERIOD ANALYSIS OF NSVS 01286630

Long-term modern photometric observations with the goal of accumulating minimum light times are necessary when using the $O-C$ method to analyze the period variation of EBs. Generally, the short-period detached EBs have deep and symmetric eclipses, which can help us to obtain individual minimum light times of mid-eclipses with high accuracy (Wolf et al. 2016).

The EB NSVS 01286630 is a newly identified EB with a precise orbital period of 0.38392787 days. Changes in eclipsing times of NSVS 01286630 were analyzed using all the minimum times published until now. During our analysis, the following linear ephemeris was

[1] IRAF is distributed by the National Optical Astronomy Observatory, which is operated by the Association of Universities for Research in Astronomy, Inc. (AURA) under cooperative agreement with the National Science Foundation.

Table 1 Coordinates of NSVS 01286630, the Comparison Star and the Check Star

Star	α_{j2000}	δ_{j2000}	$V_{\rm mag}$
NSVS 01286630	$18^{\rm h}47^{\rm m}08.59^{\rm s}$	$+78^\circ42'\ 29.2''$	13.09
Comparison	$18^{\rm h}46^{\rm m}05.37^{\rm s}$	$+78^\circ38'\ 30.2''$	13.28
Check	$18^{\rm h}47^{\rm m}23.27^{\rm s}$	$+78^\circ39'\ 46.3''$	12.76

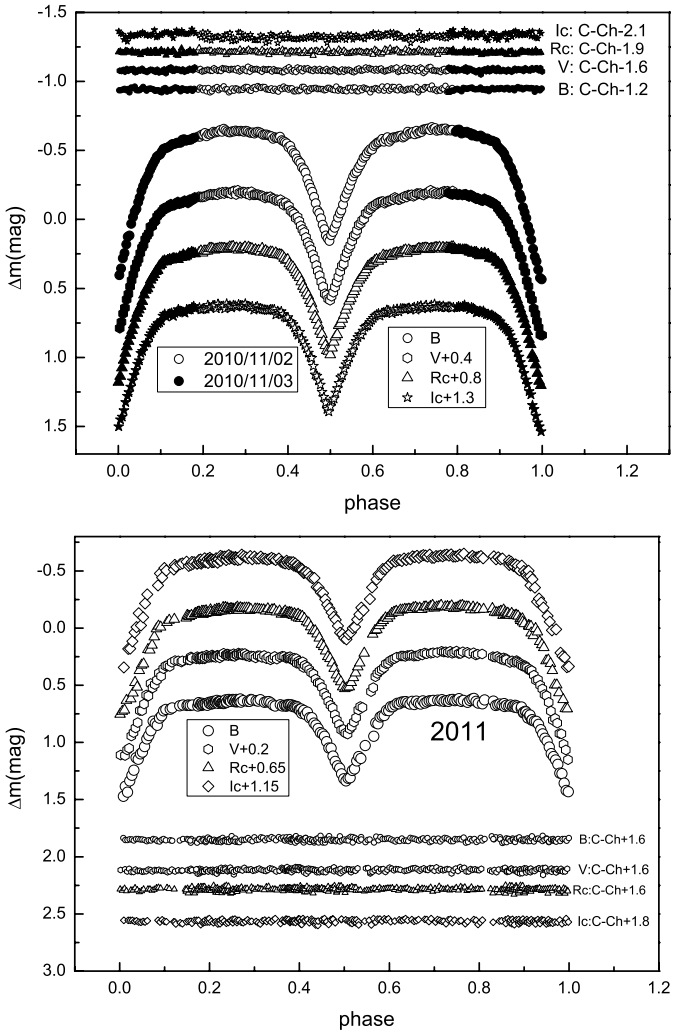

Fig. 1 LCs of NSVS 01286630 obtained in 2010 and 2011. Differential LCs of the comparison star relative to the check star are plotted and marked as $C-Ch$.

adopted

$$\begin{aligned}\mathrm{Min.(HJD)} =& 2454272.7532(\pm0.00008)\\ &+0.38392787(\pm0.00000001)^{\rm d}\times E.\end{aligned} \quad (2)$$

There are altogether 91 CCD times of light minimum that were used in our analysis, with 42 primary eclipses among them. New CCD eclipse-times of NSVS 01286630 from our observations were determined using the least-squares parabolic fitting method (Kwee & van Woerden 1956; Li et al. 2017), whose uncertainties were determined by the error propagation formula. The same minimum light times in different bands have been averaged, and only the mean values are adopted. Weights of $1/\sigma^2$ were assigned to data, where σ is error in the times of light minima. We tried several different cases for fitting the $(O-C)$ diagram, including a single sinusoidal

Table 2 New CCD Mean Times of Light Minima for NSVS 01286630

JD (Hel.)	Error (d)	Filter	Telescope
2455503.05012	±0.00040	B	85 cm
2455503.05015	±0.00034	I_c	85 cm
2455503.05024	±0.00035	R_c	85 cm
2455503.05010	±0.00040	V	85 cm
2455504.01103	±0.00039	B	85 cm
2455504.01142	±0.00061	I_c	85 cm
2455504.01138	±0.00056	R_c	85 cm
2455504.01137	±0.00050	V	85 cm
2455684.26348	±0.00043	B	85 cm
2455684.26361	±0.00049	I_c	85 cm
2455684.26382	±0.00039	R_c	85 cm
2455684.26245	±0.00041	V	85 cm
2455688.29501	±0.00018	B	85 cm
2455688.29517	±0.00024	I_c	85 cm
2455688.29491	±0.00019	R_c	85 cm
2455688.29509	±0.00025	V	85 cm
2455733.20970	±0.00063	B	85 cm
2455733.21128	±0.00045	I_c	85 cm
2455733.21062	±0.00048	R_c	85 cm
2455733.21239	±0.00057	V	85 cm
2455503.05040	±0.00037	BVR_cI_c	85 cm
2455504.01130	±0.00052	BVR_cI_c	85 cm
2455684.26334	±0.00043	BVR_cI_c	85 cm
2455688.29505	±0.00022	BVR_cI_c	85 cm
2455733.21100	±0.00063	BVR_cI_c	85 cm

function as well as a parabolic curve with a sinusoidal function. To fit the $(O-C)$ diagram well, we considered cyclic variation with eccentricity in the orbit. By considering an eccentric orbit (Irwin 1952), the fitting $(O-C)$ curve was described by the following equations:

$$\begin{aligned}(O-C) =&\Delta JD_0 + \Delta P_0 E \\ &+ A\Big[\sqrt{1-e_3^2}\sin E_3\cos\omega_3 \\ &+ \cos E_3 \sin\omega_3\Big],\end{aligned} \tag{3}$$

$$M_3 \;=\; E_3 - e_3\sin E_3 = \frac{2\pi}{P_3}(t-T_3). \tag{4}$$

In this case, the fitting residual is the smallest, and most $(O-C)$ values can be described well using these newly obtained equations, hence we accepted it as the final solution. More detailed explanation and application of equations used in the present paper can found in Liao & Qian (2010a). Two possible mechanisms can be applied to interpret this cyclical variation, the light-travel time effect (LTTE) of a third body and a magnetic activity cycle for a system with an active late-type secondary star (Applegate 1992). However, if the Applegate mechanism was working here, the mean value of period variation should be around 40–50 yr for active EBs (Wolf et al. 2016). Recently, a study that used the Kepler photometric database suggested that at least 8% of close binaries have tertiary companions with $P_{\rm trip} \leq 7$ yr, which implies that multiplicity may be a common phenomenon among close EBs (Rappaport et al. 2013). The effect of apsidal motion in eccentric EBs can also result in a quasi-sinusoidal $(O-C)$ diagram, but the resulting $(O-C)$ curves are anti-correlated between the primary minima and secondary minima (Borkovits et al. 2016). As discussed by Liao & Qian (2010b), the presence of a tertiary component around close binary systems should mainly be responsible for those variations (Zhou et al. 2016), so we think that the LTTE is the primary reason.

According to the $(O-C)$ fitting parameters, the orbital projected radius is calculated with the equation

$$a_{12}\sin i_3 = A_3 \times c, \tag{5}$$

where c is the speed of the light and A_3 is the amplitude of the $(O-C)$ oscillation, i.e., $a_{12}\sin i_3 \;=$

Table 3 The LTTE Parameters for NSVS 01286630

Element	Unit	Value (Present work)	Value (Wolf et al. 2016)
Zero epoch, T_0	HJD	2454272.75324(±0.00005)	2454272.75319(±0.00008)
Sidereal period, P_s	d	0.383927887(±0.000000013)	0.383927874(±0.000000012)
Period of third body, P_3	d	1322(±13)	1317(±15)
Eccentricity, e_3	–	0.08(±0.10)	0.17(±0.05)
ω_3	deg	342.23(±1.3)	326.4(±2.6)
Amplitude, A	d	0.00097(±0.00006)	0.00105(±0.00005)
Periastron passage, T_3	HJD	2457144.34662(±0.00010)	2454450(±15)
P_s^2/P_3	d	0.000115	0.000 11

$0.17(\pm0.01)$ AU. The mass and mass function of the tertiary companion are computed with

$$f(m) = \frac{4\pi^2}{GP_3^2} \times (a_{12}\sin i_3)^3 = \frac{(M_3 \sin i_3)^3}{(M_1+M_2+M_3)^2}, \quad (6)$$

where P_3 is the period of the $(O-C)$ oscillation and G is the gravitational constant. Finally, the best LTTE parameters and their errors are listed in Table 3. From Table 3, you can find that most parameters we obtained are very similar to the published results except for orbital eccentricity. The main reason for that is the data adopted in the analysis; during our fitting, the data with errors more than 0.00005 days were not used, however, about 112 reliable times of minimum light are included in Wolf's analysis, and some of them are not CCD measurements. It should be noted that the errors of these parameters are unbiased standard errors, and they were calculated using the degrees of freedom and the covariance matrix (Qian et al. 2015a). The $(O-C)$ diagram and residuals for all data with respect to the above-mentioned linear ephemeris are shown in Figure 2.

4 PHOTOMETRIC SOLUTIONS WITH W–D PROGRAM

The first photometric solutions of NSVS 01286630 in V, R and I bands were published in 2007. In order to check these photometric elements and understand this star's evolution state, we intend to analyze the present new LCs in BVR_cI_c bands with the 2013 version of the Wilson-Devinney (W–D) code (Wilson & Devinney 1971; Wilson 1979, 2012). Before using the W–D code, we set the initial values for some fixed parameters. The possible effective temperature for the primary component (star 1), $T_1 = 4290$ K, was fixed according to average color index. The same value of gravity-darkening coefficients is taken, i.e., $g_1 = g_2 = 0.32$ (Claret 2000), and the bolometric albedos for both components were set as $A_1 = A_2 = 0.5$ (Ruciński 1969). The orbital eccentricity $e = 0$, since when the orbital period is less than 1 day, close binary orbits become circularized (Zahn 1989). The adjustable parameters are: mean effective temperature of the secondary component, T_2; mass ratio, q; monochromatic light of star 1, L_{1B}, L_{1V}, L_{1R_c} and L_{1I_c}; orbital inclination, i; dimensionless potentials of the two components, Ω_1 and Ω_2.

As is well known, a reliable mass ratio of EBs can be directly constrained by high quality radial velocities (Becker et al. 2008). The magnitude of NSVS 01286630 in the V-band is about 13.1 mag (Hoffman et al. 2008). Fundamental parameters can be determined with high signal-to-noise ratio (>10) spectra, but this will require at least a 4 m class telescope, which is difficult for us now. Besides, because there are no spectroscopic observations for NSVS 01286630 published up to now, we used a q-search method (with fixed q) to obtain initial input parameters. During this process, we added a third light considering the fitting results of the $(O-C)$ diagram. From Figure 1, we can see that the LCs observed in 2010 are of better quality, so we started the analysis with this set of LCs. Using the grid computing method, a range from 0.5 to 3 (with a step of 0.1) was explored, however, when the value of mass ratio was less than 0.5 we could not find a convergent solution. During the calculation, it was found that the solutions converged at mode 2 (for detached binaries) in the end. The q-search result for NSVS 01286630 is shown in Figure 3, and the optimal mass ratio we found was $q = 1.5$. After that, we treated q as a free parameter and set its initial value to be 1.5. Then, one set of solutions would be derived when running the W–D code over and over again until all free parameters converged, although when adopting the

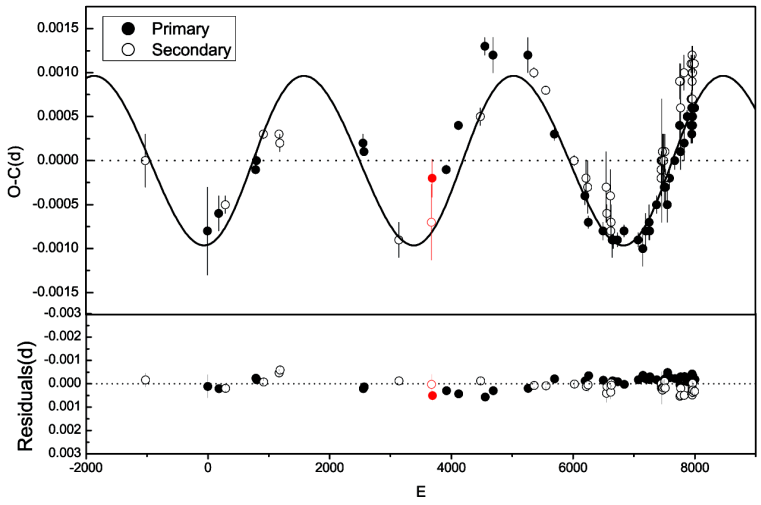

Fig. 2 The $(O-C)$ diagram of NSVS 01286630 formed by all available measurements with the linear ephemeris provided in Equation (2). *Open circles* and *dots* refer to the secondary and primary CCD minimum light times with error bars respectively. The *sine curve* represents cyclic variation, and the line signifies linear variation. The corresponding $(O-C)$ residuals are shown in the bottom panel.

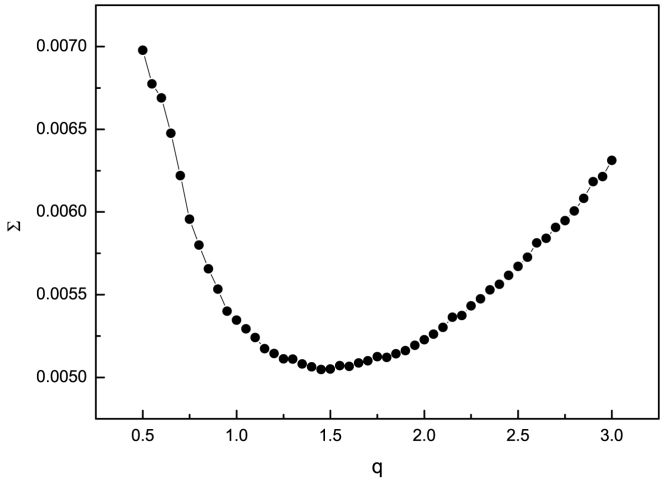

Fig. 3 The $\Sigma - q$ curves for NSVS 01286630 derived with BVR_cI_c-band LCs in 2010. The optimal value of mass ratio is $q = 1.5$.

optimal mass ratio, the fitting results are still not good when the star is outside of eclipses. In view of this case, a cool starspot model was adopted to fit the observed LCs (Zhang et al. 2018). After many attempts, we found that one spot on the surface of the primary component and another one on the surface of the secondary component could fit the LCs pretty well, reducing the residual by 60%. This means that the two components of NSVS 01286630 are active stars with cool starspots. This case is similar to NSVS 11868841 the study results of which were published several years ago (Çakirli et al. 2010). At the same time, it should be noted that both of these cool starspots are near the polar field.

According to the same process as stated above, we analyzed the LCs from 2011 using the W–D code again. A similar spotted scenario is adopted in the final solutions and the $\Sigma - q$ curves are generally the same as the former. However, the solutions are found to be have some differences as compared to the former, which can be caused by changes in the shape of observed LCs. Finally, after a detailed comparison, the best photometric solutions are listed in Table 4. However it should

Table 4 Photometric solutions for NSVS 01286630

Parameter	This paper 2010	This Paper 2011
$g_1 = g_2$	0.32	0.32
$A_1 = A_2$	0.5	0.5
T_1 (K)	4290	4290
q	1.12(±0.10)	1.15(±0.15)
T_2/T_1	0.9697(±23)	0.9655(±58)
i (°)	89.814(±0.167)	89.917(±0.058)
$L_1/(L_1+L_2)(B)$	0.5678(±0.0040)	0.5509(±0.0150)
$L_1/(L_1+L_2)(V)$	0.5544(±0.0035)	0.5357(±0.0121)
$L_1/(L_1+L_2)(R_c)$	0.5448(±0.0038)	0.5256(±0.0122)
$L_1/(L_1+L_2)(I_c)$	0.5353(±0.0042)	0.5146(±0.0126)
$L_3/(L_{\rm all})(B)$	0.0048(±0.0002)	0.0044(±0.0002)
$L_3/(L_{\rm all})(V)$	0.0062(±0.0002)	0.0058(±0.0002)
$L_3/(L_{\rm all})(R_c)$	0.0082(±0.0003)	0.0078(±0.0003)
$L_3/(L_{\rm all})(i_c)$	0.0295(±0.0004)	0.0361(±0.0006)
Ω_1	4.077(±0.025)	4.183(±0.037)
Ω_2	4.204(±0.030)	4.201(±0.028)
r_1 (pole)	0.3315(±0.0010)	0.3226(±0.0038)
r_1 (point)	0.4026(±0.0030)	0.3826(±0.0091)
r_1 (side)	0.3455(±0.0012)	0.3353(±0.0044)
r_1 (back)	0.3700(±0.0016)	0.3574(±0.0058)
r_2 (pole)	0.3375(±0.0040)	0.3455(±0.0028)
r_2 (point)	0.3936(±0.0052)	0.4094(±0.0068)
r_2 (side)	0.3509(±0.0044)	0.3602(±0.0033)
r_2 (back)	0.3710(±0.0060)	0.3820(±0.0042)
θ_s (°)	P:292.574(±2.349)	P:27.275(±5.157)
	S:129.90(±2.865)	S:117.465(±6.016)
ψ_s (°)	P:114.94(±1.490)	P:71.338(±4.240)
	S:277.447(±0.974)	S:94.946(±1.489)
r_s (°)	21.6(±0.12), 24.87(±0.17)	23.32(±0.25), 24.92(±0.28)
T_s/T_*	0.86, 0.85	0.86, 0.85
$\sum (O-C)_i^2$	0.00178	0.00410

Notes: $L_{\rm all} = L_1 + L_2 + L_3$, P refers to the primary component, S means the secondary one.

be noted that the listed errors calculated with the W–D code are only probable errors (Liu et al. 2015). These errors are obtained in nonlinear situations, and because of complex correlations among the full set of parameters (Wilson & Biermann 1976), the real parameter uncertainties may be three to five times larger than what the W–D code provided (Popper 1984; Abubekerov et al. 2009). The theoretical LCs are plotted in Figure 4. The geometrical structure of the system at different phases is displayed in Figure 5.

5 DISCUSSION AND CONCLUSIONS

First, four-color LC solutions for NSVS 01286630 are obtained using the 2013 version of the W–D code. Due to the asymmetry of these LCs, a cool starspot model is used to analyze the LCs for better determination of basic orbital parameters. The photometric solutions are relatively reliable considering an inclination of nearly 90°. The difference between two sets of photometric solutions may be caused by the evolution of the cool starspots. The solutions from both sets of LCs suggest that NSVS 01286630 is an active detached EB system with a small temperature difference. Moreover, the photometric solutions show that the value of mass ratio $q(\frac{M_2}{M_1})$ is more than 1, which is a very different value compared with other late-type detached binaries (Torres & Ribas 2002; Morales et al. 2009). The main reason for this may be the presence of big cool starspots on the secondary component of NSVS 01286630. Our photometric solutions

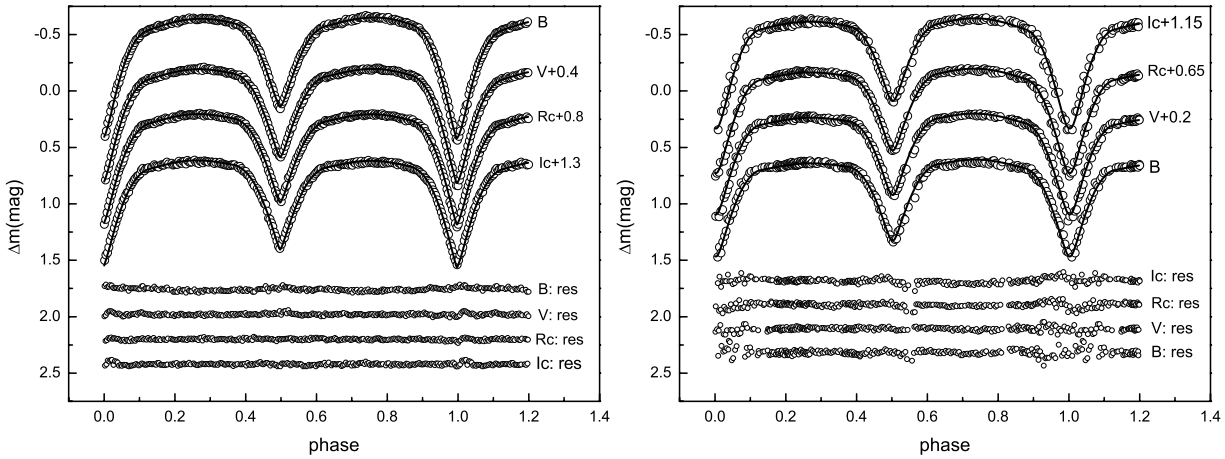

Fig. 4 The two sets of observational and theoretical LCs for NSVS 01286630 in BVR_cI_c bands. The different *hollow symbols* and *solid lines* represent the observational and theoretical LCs, respectively. Corresponding residuals between observed LCs and theoretical fits are plotted in the bottom of each panel.

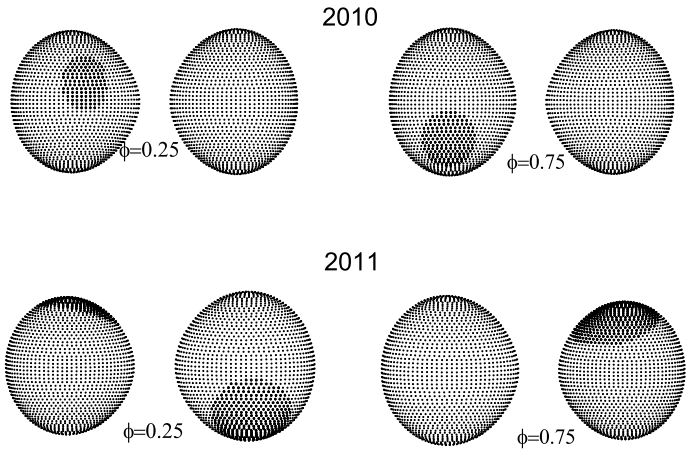

Fig. 5 Geometric configurations of NSVS 01286630 at different phases in 2010 and 2011.

suggest that the coverage of cool starspots on the surface of the secondary component is about 5% (2010) and 11% (2011). Usually, late-type stars with a deeper convective envelope and faster rotation will, in turn, produce a strong magnetic field (Claret. 2000; Zhang et al. 2014). With a strong magnetic field and sufficient internal convection, the radius of these late-type low-mass stars could inflate while at the same time the surface effective temperature decreases (Chabrier & Baraffe 2000; Morales et al. 2010).

The most striking feature of this binary system is its starspot activity. Therefore, the photometric solutions with cool starspots was adopted. The surface cool starspots can make the observed LCs distorted, especially in shorter wavelengths ($U-$, $B-$ and $V-$bands), such as what is observed in CU Cnc (Qian et al. 2012). Generally, the cool starspots tend to occur around some longitude, forming active longitude belts (Lanza et al. 2002; Çakırlı et al. 2003). The main features of these longitudes are permanent activity and continuous migration (Berdyugina & Tuominen 1998; Berdyugina 2005). As previously emphasized, the cool starspots we obtained were near polar regions, which are listed at the bottom of Table 4. According to the dynamo mechanism, the magnetic field of a late-type star is similar to a magnetic dipole, which manifests a stronger magnetic field intensity near the polar regions than other locations considering its rotation (Durney & Robinson 1982). Therefore, stars that are fast rotators are more likely to exhibit cool starspots at high latitudes and polar regions (Schuessler & Solanki 1992). More importantly, the tidal effects can result in evolution of cool starspots

along with the active longitudes and emerge on the surface (Zhang et al. 2014). Tran et al. (2013) suggest that a cool starspot is continuously visible around the orbit and slowly changes its longitude on timescales of weeks to months. This is the reason why the two sets of parameters for cool starspots we obtained are somewhat different. Similar late-type detached binaries include NSVS 02502726 (Lee et al. 2013); NSVS 10653195 (Zhang et al. 2015); NSVS 6507557 (Ćakırlı & Ibanoğlu 2010) and NSVS 07453183 (Zhang et al. 2014).

The $(O-C)$ diagram of NSVS 01286630 shows typical cyclical variation, which may be caused by the presence of a third body or the magnetic activity from one or both components (Applegate 1992). If such magnetic activity is operating, variations in the gravitational quadrupole moment (ΔQ) may result in observed oscillations. By using the formula $\Delta P/P = 9\Delta Q/Ma^2 = 2\pi A/P_{\rm mod}$ (Lanza & Rodonò 2002), where M is the mass of the active component and a is the separation between both components (Yang et al. 2012), we can compute the values as follows: $\Delta Q_1 = 9.64\times10^{48}$ g cm^2 and $\Delta Q_2 = 1.14\times10^{49}$ g cm^2. These are evidently smaller than the typical values of 10^{51}–10^{52} g cm^2 for close binaries (Lanza & Rodonò 1999). Therefore, we can rule out Applegate's mechanism for interpreting the cyclic variations of NSVS 01286630 (Yang et al. 2014). Hence, NSVS 01286630 may be a triple system. Based on fitting parameters from the $(O-C)$ diagram, we can estimate the mass of the third body to be $M_3\sin(i_3) = 0.11\,M_\odot$, and the distance of the binary system to the barycenter of the triple system is calculated to be $a_{12}\sin(i_3) = 0.17(\pm0.01)$ AU. In this case, the distance of the third body to the barycenter of the triple system can be calculated to be $a_3\sin(i_3) = 2.38$ AU. As yet, however, the data adopted in our analysis just span 10 yr, so further observations are required to verify the oscillation observed by us.

NSVS 01286630 is a detached close EB in which neither component is filling the critical Roche lobe now. It will evolve into a short-period W UMa-type binary until the components fill their critical Roche lobe. So far, the formation and evolution of short-period W UMa-type binaries are still an unsolved problem in astrophysics, and NSVS 01286630 offers as good an example as DV Psc (Zhang & Zhang 2007) for studying this process. Some researchers (Liao & Qian 2010b; Torres & Ribas 2002) surveyed many EB systems with modern photometric analysis and found that many close binaries have additional companions. The spectral type of these binaries ranged from B to M, and more than half of them are late-type EBs. However, their origin is still questionable in several cases. One theory suggests that an intensive dynamic interaction process between the binary system and these close-in stellar companions may change the formation and evolutional path of these stars. For example, the third body might extract angular momentum from the central binary system during early dynamical interaction or late evolution (Qian et al. 2014). As a result, the third body may help to shorten the time of orbital evolution for these central binary systems (Fabrycky & Tremaine 2007; Zhou et al. 2016).

Acknowledgements This work is partly supported by the National Natural Science Foundation of China (Nos. 11573063, 11611530685) and the Key Science Foundation of Yunnan Province (No. 2017FA001). We acknowledge support from the staff of the Xinglong 85 cm telescope, and this work was partially supported by the Open Project Program of the Key Laboratory of Optical Astronomy, National Astronomical Observatories, Chinese Academy of Sciences.

References

Abubekerov, M. K., Gostev, N. Y., & Cherepashchuk, A. M. 2009, Astronomy Reports, 53, 722
Applegate, J. H. 1992, ApJ, 385, 621
Bai, C., Fu, J., Li, T., et al. 2018, RAA (Research in Astronomy and Astrophysics), 18, 107
Becker, A. C., Agol, E., Silvestri, N. M., et al. 2008, MNRAS, 386, 416
Berdyugina, S. V., & Tuominen, I. 1998, A&A, 336, L25
Berdyugina, S. V. 2005, Living Reviews in Solar Physics, 2, 8
Borkovits, T., Rappaport, S., Hajdu, T., & Sztakovics, J. 2015, MNRAS, 448, 946
Borkovits, T., Hajdu, T., Sztakovics, J., et al. 2016, MNRAS, 455, 4136
Çakirli, Ö., Ibanoglu, C., & Dervisoglu, A. 2010, RMxAA, 46, 363
Çakırlı, Ö., İbanoğlu, C., Djurašević, G., et al. 2003, A&A, 405, 733
Ćakırlı, Ö., & Ibanoğlu, C. 2010, MNRAS, 401, 1141
Chabrier, G., & Baraffe, I. 2000, ARA&A, 38, 337
Claret, A. 2000, A&A, 359, 289
Conroy, K. E., Prša, A., Stassun, K. G., et al. 2014, AJ, 147, 45
Coughlin, J. L., & Shaw, J. S. 2007, Journal of the Southeastern Association for Research in Astronomy, 1, 7

Durney, B. R., & Robinson, R. D. 1982, ApJ, 253, 290
Fabrycky, D., & Tremaine, S. 2007, ApJ, 669, 1298
Gies, D. R., Williams, S. J., Matson, R. A., et al. 2012, AJ, 143, 137
Hoffman, D. I., Harrison, T. E., Coughlin, J. L., et al. 2008, AJ, 136, 1067
Irwin, J. B. 1952, ApJ, 116, 211
Kwee, K. K., & van Woerden, H. 1956, Bull. Astron. Inst. Netherlands, 12, 327
Lacy, C. H. 1977, ApJS, 34, 479
Lanza, A. F., Catalano, S., Rodonò, M., et al. 2002, A&A, 386, 583
Lanza, A. F., & Rodonò, M. 1999, A&A, 349, 887
Lanza, A. F., & Rodonò, M. 2002, Astronomische Nachrichten, 323, 424
Lee, J. W., Youn, J.-H., Kim, S.-L., & Lee, C.-U. 2013, AJ, 145, 16
Lee, J. W., Hong, K., Koo, J.-R., & Park, J.-H. 2016, ApJ, 820, 1
Li, K., Hu, S., Zhou, J., et al. 2017, PASJ, 69, 28
Li, L.-J., & Qian, S.-B. 2014, MNRAS, 444, 600
Liao, W.-P., & Qian, S.-B. 2010a, PASJ, 62, 1109
Liao, W.-P., & Qian, S.-B. 2010b, MNRAS, 405, 1930
Liu, N.-P., Qian, S.-B., Soonthornthum, B., et al. 2015, AJ, 149, 148
Morales, J. C., Ribas, I., Jordi, C., et al. 2009, ApJ, 691, 1400
Morales, J. C., Gallardo, J., Ribas, I., et al. 2010, ApJ, 718, 502
Popper, D. M. 1984, AJ, 89, 132
Qian, S.-B., Zhang, J., Zhu, L.-Y., et al. 2012, MNRAS, 423, 3646
Qian, S.-B., Zhou, X., Zola, S., et al. 2014, AJ, 148, 79
Qian, S.-B., Li, L.-J., Wang, S.-M., et al. 2015a, AJ, 149, 4
Qian, S.-B., Jiang, L.-Q., Fernández Lajús, E., et al. 2015b, ApJ, 798, L42
Qian, S.-B., He, J.-J., Zhang, J., et al. 2017, RAA (Research in Astronomy and Astrophysics), 17, 087
Rappaport, S., Deck, K., Levine, A., et al. 2013, ApJ, 768, 33
Ruciński, S. M. 1969, Acta Astronomica, 19, 245
Schuessler, M., & Solanki, S. K. 1992, A&A, 264, L13
Torres, G., & Ribas, I. 2002, ApJ, 567, 1140
Tran, K., Levine, A., Rappaport, S., et al. 2013, ApJ, 774, 81
Wilson, R. E. 1979, ApJ, 234, 1054
Wilson, R. E. 2012, AJ, 144, 73
Wilson, R. E., & Devinney, E. J. 1971, ApJ, 166, 605
Wilson, R. E., & Biermann, P. 1976, A&A, 48, 349
Wolf, M., Zasche, P., Kučáková, H., et al. 2016, A&A, 587, A82
Woźniak, P. R., Vestrand, W. T., Akerlof, C. W., et al. 2004, AJ, 127, 2436
Yang, Y.-G., Yang, Y., & Li, S.-Z. 2014, AJ, 147, 145
Yang, Y.-G., Zhang, X.-B., Li, H.-L., & Dai, H.-F. 2012, AJ, 144, 136
Zahn, J.-P. 1989, A&A, 220, 112
Zasche, P., Wolf, M., Kučáková, H., et al. 2015, AJ, 149, 197
Zhang, B., Qian, S.-B., Liao, W.-P., et al. 2015, New Astron., 41, 37
Zhang, B., Qian, S.-B., Michel, R., Soonthornthum, B., & Zhu, L.-Y. 2018, RAA (Research in Astronomy and Astrophysics), 18, 030
Zhang, L.-Y., Pi, Q.-f., & Yang, Y.-G. 2014, MNRAS, 442, 2620
Zhang, X. B., & Zhang, R. X. 2007, MNRAS, 382, 1133
Zhou, A.-Y., Jiang, X.-J., Zhang, Y.-P., & Wei, J.-Y. 2009, RAA (Research in Astronomy and Astrophysics), 9, 349
Zhou, X., Qian, S.-B., Zhang, J., et al. 2016, ApJ, 817, 133
Zhu, L.-Y., Qian, S.-B., Zhou, X., et al. 2013, AJ, 146, 28